Polarisation gain terms for LBA data.
eLBA memo 9

R Dodson

University of Western Australia

Contents

I : Abstract

I have reported elsewhere on the development of new code to support the Nasmyth and E-W antenna mount types in AIPS which will allow polarisation analysis of observations made using these uncommon antenna configurations [**?**]. In this report I underline the aspects of particular relevance to the LBA, and in particular Hobart which has an EW mount. The new generation of geodetic arrays as discussed in IVS2010 are required to have very high slew rates, and these can be achieved with the E-W mount. Therefore it is possible that this mount will become significantly more popular.

Any mount type affects the differential phase between the left and the right hand circular polarisations (LHC and RHC) for different points on the sky. The routines in AIPS correct for the predictable phase differences between LHC and RHC. Equatorial and Cassegrain mounts were supported. The new additions are EW-and Nasmyth (left and right) mounts.

II : Telescope Mounts

Mount types are a combination of the focus position and the drive type. In Radio Astronomy there are six more or less commonly used focus positions, and three drive types.

II.1 Focus positions

Radio telescopes use a much more limited set of focus positions compared to optical telescopes. Here we list them, along with examples of the codes for telescopes which use them (in brackets). Images of these are shown in figure 1 and a general schematic is shown in figure 2.

- Prime focus (PKS). Focus at the site of the secondary mirror (sub-reflector).

- Cassegrain focus (VLBA/most). Focus after the secondary (hyperboloid) mirror.

- Gregorian focus (EFF). Prime Focus before the secondary (ellipsoid) mirror, secondary focus after the secondary mirror.

- Folded Cassegrain focus (CED). Focus bolted to the elevation axis, after the tertiary mirror.

- Reduced Nasmyth focus (JCMT). Focus on the elevation axis, but bolted to the azimuth floor, after the tertiary mirror.

- Full Nasmyth focus (YEB40). Focus bolted to the azimuth axis floor, after the forth mirror.
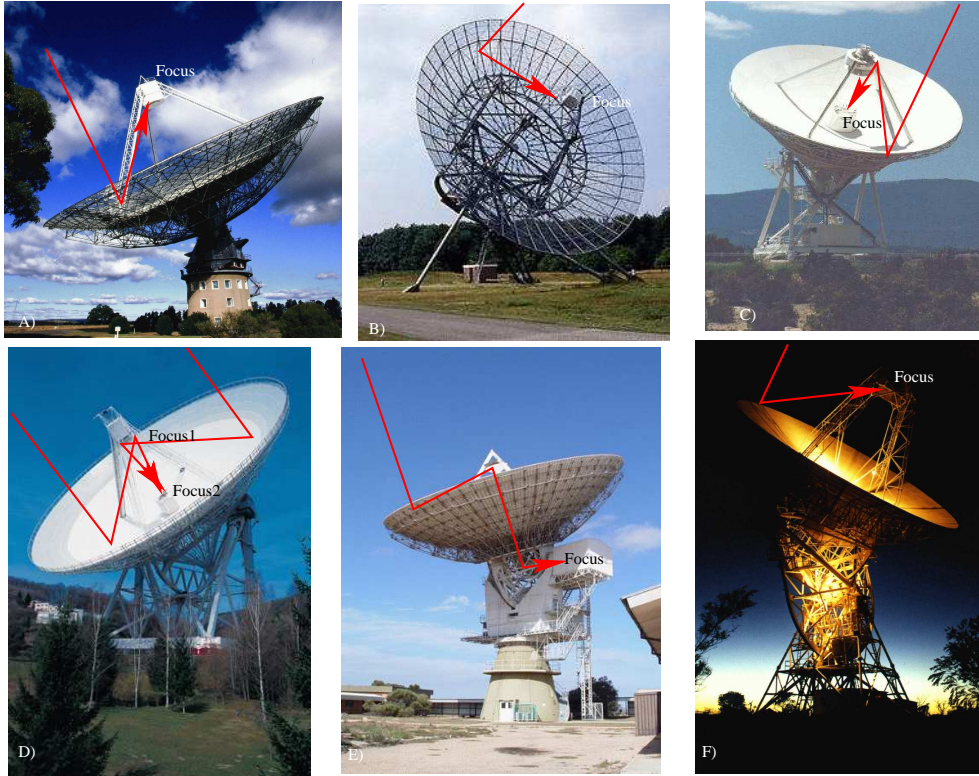
Figure 1: A montage of different antennae displaying different focus positions and drive types. A) Parkes (NSW, Australia). Prime focus, Alt-Az drive, B) Westerborg (Holland). Prime focus, HA-Dec drive. C) Los Alamos (USA). Cassegrain focus, Alt-Az drive. D) Effelsberg (Germany) Either Prime or Gregorian focus, Alt-Az drive. E) Ceduna (SA. Australia). Folded Cassegrain focus, Alt-Az drive. F) Hobart (TAS Australia) Prime Focus, EW drive.

Mirrors after the forth, in a Nasmyth system, swap the mount type between the equivalent of a reduced and full Nasmyth, so that any system with an odd number of mirrors is a 'reduced' and an even number of mirrors is equivalent to a 'full' Nasmyth system in our context. In a similar fashion the expression for a folded Cassegrain and Prime focus solutions are essentially the same, being either one or three reflections from the on-sky view. The difference between a Cassegrain and a Gregorian image is a rotation (of 180°) so these types are degenerate after the absolute position angle calibration. Furthermore at the correlator, the 'on sky' left or right is combined with the same to produce the parallel hand output. This is effectively the same as adding another mirror to the optical chain for those optics with an odd number of mirrors. However the M3 (at the Cassegrain focus) mirror can reflect to the right or left. The left-handed and right-handed solutions are different. For all expected cases, therefore, we will be correlating either Cassegrain or Nasmyth foci, combined with the drive type of the antenna.

Elevation Axis

M1

Telescope Axis

Cassegrain

Primary Focus

M3

M2

M4

Full Nasmyth

Reduced Nasmyth or
Folded Cassegrain
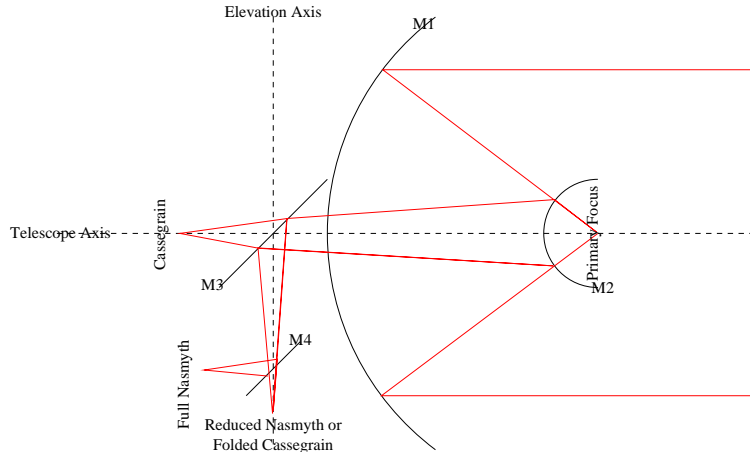
Figure 2: Mount types

II.2 Drive configuration

There are three drive configurations used in VLBI. This also effects the rotation of the feeds as seen from the sky.

- HA-DEC (WST), for Hour Angle – Declination. Also called equatorial. It produces no change of feed angle as the source passes across the sky. As HA-DEC mounts require an asymmetrical structural design they are unsuited to the support of very heavy structures. Their advantage is that motion is required in only one axis to track an object as Earth rotates.

- ALT-AZ (VLBA/most), for Altitude – Azimuth. Also called Az-El. It rotates the telescope pointing by the parallactic angle as the source passes across the sky. It is the most common variety of Radio telescope mount. It is symmetric so can support very large antennae, but at the zenith small angular changes on the sky can require very large angular changes in the azimuth angle. This effect is call the 'keyhole'.

- EW (HOB), for East – West. It rotates the telescope by the co-parallactic angle as the source passes across the sky. An EW mount places the focus very high, therefore it is prone to flexing and poor pointing. Their advantage is that they can track across the sky at high speeds and without gaps (i.e. it does not have a 'keyhole' at the zenith). They are designed for tracking Low Earth Orbit satellites.

The parallactic angle, sometimes called the position angle, of an object is the angle between the celestial pole (north or south depending on location), the object and the zenith (the point in the sky directly overhead). It is not to be confused for the same named angle which is also called the convergence angle. This is the difference

in the angular direction to an object at a distance, from two points of view, i.e. the parallax. The expression for the parallactic angle as we use it is;

$$\chi_p = \arctan[\frac{\sin(\Theta)\,\cos(l)}{\cos(\delta)\sin(l) - \cos(\Theta)\cos(l)\sin(\delta)}]$$

The co-parallactic angle is;

$$\chi_c = \arctan[\frac{\cos(\Theta)}{\sin(\delta)\sin(\Theta)}]$$

The Nasmyth angle is almost the same as the parallactic angle, but with the relative rotation of the third mirror included;

$$\chi_n = \chi_p \pm E$$

where Θ is the hour angle, and δ the declination, of the source. l is the latitude of the telescope and E is the elevation.

III : AIPS code changes

The AIPS code was changed to add support for the Nasmyth and EW-mount optics as well as the traditional Equatorial and Cassegrain. The core subroutine for the calculation of parallactic angles was extended to return either, the parallactic plus or minus the elevation angles, or co-parallactic angles (i.e. the correct formalisation for these mount types). The mount types, and their numeric values, are listed in table 1. All angles are calculated in the code using the function **atan2** to allow the full range of angles to be returned.

Focus and Drive	Label	Mount Number Final
Cassegrain and Alt-Az	ALAZ	0
Any and Equatorial	EQUA	1
Any and Orbiting	ORBI	2
New mount types		
Prime focus and EW	EW--	3
Right hand Naysmyth and Alt-Az	NS-R	4
Left hand Naysmyth and Alt-Az	NS-L	5

Table 1: Mount Types

All calls to this code have been checked, as have all calls to the mount type via GETAN, all mentions of "parallactic" in the source code, and all mentions of any of the common names for mount type (MNTYP, MNTSTA, MNTEL and IDTMNT). All issues associated with those have been fixed. A full list of the differences can be found in appendix B.

The greatest problem was that not all derivations of the parallactic angle were done with a single common subroutine. This was fixed for most cases, but in one case it has not been standardised, i.e. VPLOT (for which one can use UVPLT). In VPLOT the position angle is only used as an alternative plotting axis, and therefore has no impact on the data reduction.

IV : Data visualisation

The first stage of calibration is to correct the relative phase rotation between the left hand and the right hand receivers. The success of this stage can be easily demonstrated with the task VPLOT by plotting the phases difference between the two polarisations (usually against time). The phase of the ratio of the parallel hands will be, before feed angle calibration;

$$\frac{R_1 R_2}{L_1 L_2} = \frac{g_{R_1} g_{R_2}^*}{g_{L_1} g_{L_2}^*} e^{-i(\chi_1 - \chi_2)}$$

and after;

$$\frac{R_1 R_2}{L_1 L_2} = \frac{g'_{R_1} g'^*_{R_2}}{g'_{L_1} g'^*_{L_2}}$$

Therefore the phases between the two polarisations, post feed angle calibration, will have a constant phase. See figure 3 here and in 6 and 12 in Dodson (2007). Post phase calibration, of course, this phase will be zero. This step is in theory independent of any other calibration but in practice, as the data is averaged then compared, the delays need to be solved for and the VPLOT averaging has to be less than the (post-calibration) coherence time. That is, either short averaging intervals must be used (with the risk that the phase difference will be undetectable) or at least some phase calibration must have been performed. It is important that, in this case, the phases applied to each polarisation are not independent. Otherwise the effect is masked as the phases are absorbed into the calibration.

Conventionally the quality of the polarisation solutions was judged from plotting RL/RR (or LR or against LL) on the real/imaginary plane with and without polarisation calibration. Without calibration the values will fall on a circle around an (offset and potentially moving) origin, as a function of feed angle difference, following:

$$RL/RR = p e^{-2i\chi_2} + D_{L_2}^* + D_{R_1} e^{2i(\chi_1 - \chi_2)}$$

I.e. if the source is unpolarised ($p = 0$), the centre is $D_{L_2}^*$ and the radius of the circle is D_{R_1}.
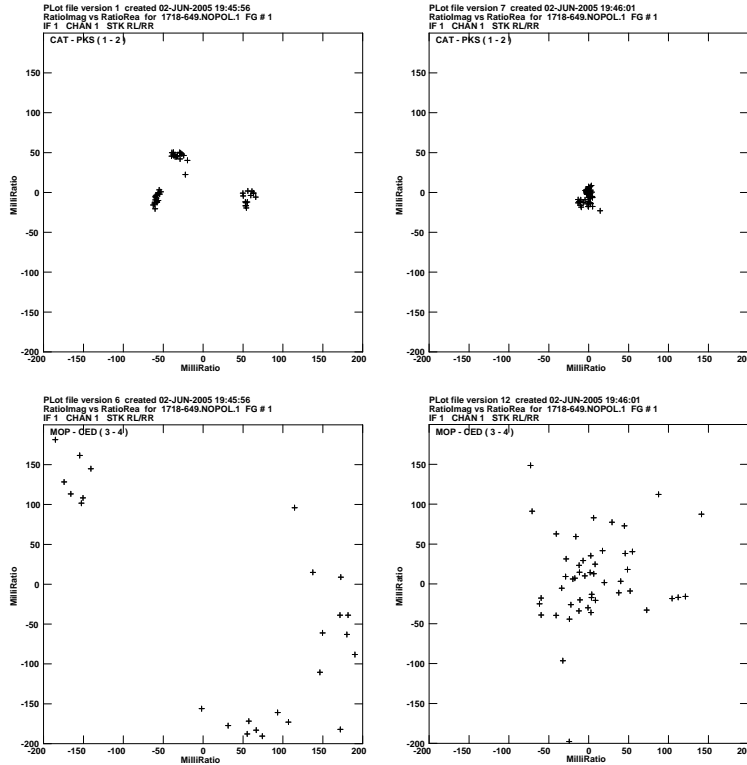
Figure 3: Pre- and Post- polarisation solution from traditional VPLOT display for the four antennae in V148A.

V : Some demonstrations from the LBA

V.1   V182

This experiment was performed at 4.8 GHz with 64 channels of about 0.25 MHz each. The target source (J0743-67) is an AGN with an interesting double structure. The calibrator was J0637-752, also an interesting source. It was the first experiment to produce solutions for the polarisation on the LBA, but was not designed as a polarisation experiment, therefore it did not include a absolute polarisation calibrator and all position angles are arbitrary. It included Hartebeesthoek so had more baselines to solve for amplitude and D-terms. Reduction followed the standard routes, apart from changing the mount types to EW mount for Hobart and equatorial mount for Hartebeesthoek.

V.2   V148

This experiment was a 6.7 GHz polarisation experiment with Parkes (Prime focus), ATCA and Mopra (Cassegrain), Ceduna (Folded Cassegrain) and Hobart (E-W
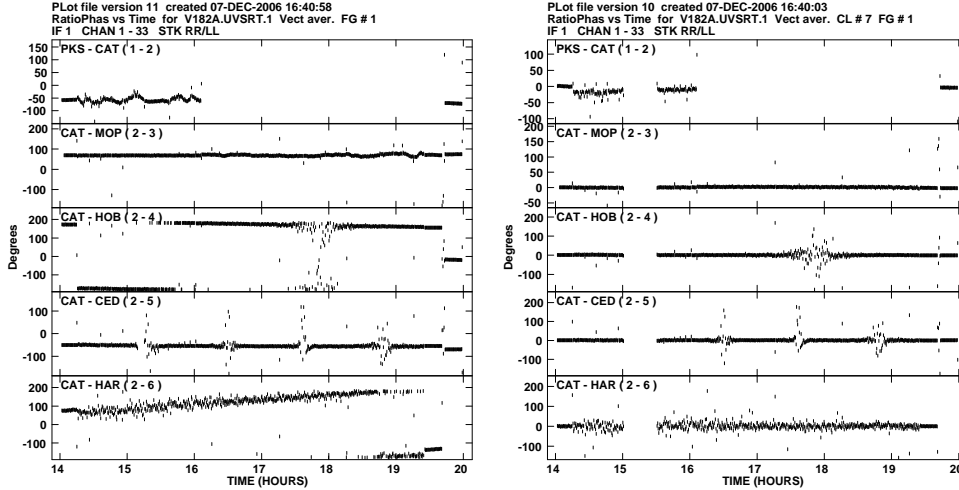
Figure 4: The RR/LL phase difference in LBA experiment V182A before and after feed angle correction types. The mount types are parallactic and equatorial and co-parallactic. The phase between the two polarisations before (left) and after removal of the feed rotation in V182A, for all antennae to the CAT. The rotation of the feeds introduces a variable phase between the two hands in the data. The effect of the near identical feed angles for the NSW antenna is indicated by the near constant phases between them. The phases are flattened (and zeroed for the calibrator at 14UT) for all antennae in the corrected data, which is shown on the right.

mount). It was in two session (A1+A2 and B) in 2001 and included seven scans each of two polarisation calibrators (1610-771 and 1718-649). After calibration we could sum across the VLBI image and compare it to a similarly summed ATCA image (from 2000). Figure 6 shows the comparison, which proves that the solutions were consistent. More details are to be found in Dodson (2008).

V.3   VX014A

Four sources were observed in VX014, of which two are in the MOJAVE program (Lister & Homan, 2005); the Monitoring Of Jets and AGNs with VLBA Experiments. We compared the images of these two sources, 3C273 and 3C279, despite the differences in resolution and frequency between the two observations. The LBA at 8.4-GHz has a resolution of $\sim$3 mas and the VLBA at 15-GHz has a resolution of $\sim$0.5 mas. Nevertheless we smoothed the VLBA images to the resolution of the LBA, and amplitude scaled the LBA data to match the fluxes; assuming a simple spectral index between the two frequencies. With these simple corrections the total power images from the two instruments are in very good agreement, giving us the confidence to compare the polarisation.

The images in Figure 7 show the total power, with a log scaled colour index. Over-

9
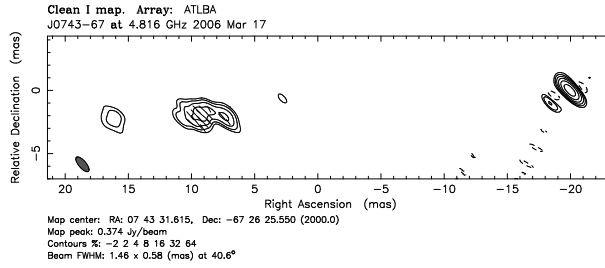
Figure 5: The image of J0743-67 from experiment V182A. The polarisation vectors are shown overlaid. Absolute polarisation angles can not be derived so the direction is arbitrary. The core (to the West) is unpolarised ($\leq 1\%$) and the jet (to the East) is smoothly polarised with a polarised fraction of approximately 16%.
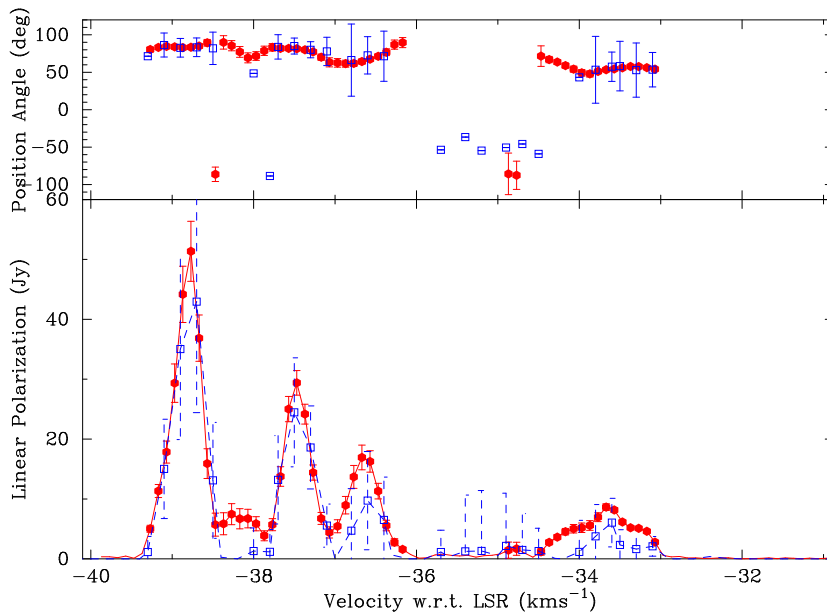
Figure 6: Polarisation angle and fraction for G339-1.26, as observed by the LBA (this paper, blue open squares) and the ATCA (Ellingsen, priv. comm., red closed circles). The spectra is scalar summed across the image (Stokes I,Q and U), and shows good agreement between the VLBI and the connected array results. The errors are the absolute errors based on the confidence in the polarisation calibration (2% and 0.4% respectively), not the relative errors. Where errors are not shown they could not be calculated. From Dodson, 2007

10
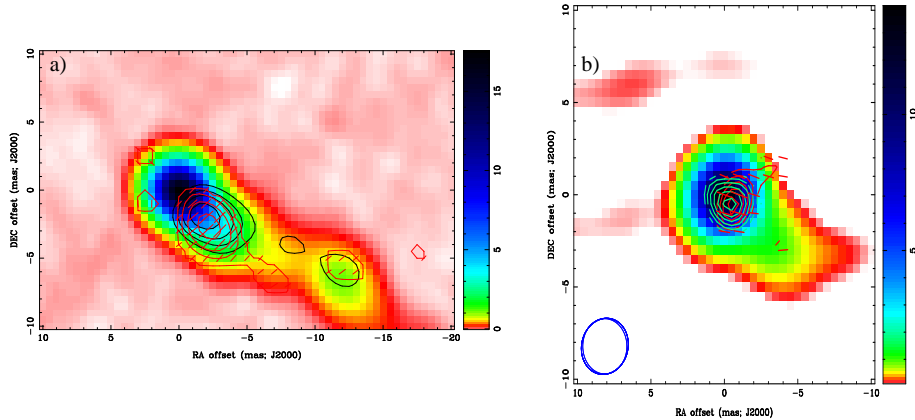
Figure 7: The polarised flux from 3C273, as observed by the LBA and the VLBA in 2008. The colour scale is the LBA total intensity, the black contours are the VLBA polarised intensity, the red those of the LBA with the LBA polarisation vectors overlaid. b) The polarised flux from 3C279, as observed by the LBA and the VLBA in 2008. The colour scale is the LBA total intensity, the blue contours are the VLBA polarised intensity, the red those of the LBA with the LBA polarisation vectors overlaid.

laid are the contours from the linear polarised flux for LBA and VLBA data. The vectors are the field directions for the LBA data, these are in good agreement with those of the VLBA data. However this is not total independent, as the VLBA image was used to provide the calibration in LPCAL. The D-term solutions for the two sources (both assuming a polarised source and an unpolarised source) were in agreement to a few percent, dominated by the errors in Mopra. It is notable to the first order that there is a good match between the results from the LBA and the VLBA, but at the second order there are notable differences. These will need further investigation, as it is possible that they are due to the second order effects from the very high polarisation feed correction in the LBA calibration terms. Work is undergoing to improve these, particularly for Mopra, which were known to be anomalous.

VI : Recommendations for the scheduling of polarisation observations

A conventional polarisation experiment should have the target, secondary and primary calibrators, as normal. In addition one would normally have regular observations of a D-term (polarisation) calibrator and an absolute polarisation angle calibrator. With the compact array I believe one maybe able to skip the latter as the calibrator polarisation (as long as it is polarised of course) can be measured at

the CA and the polarisation angle in the (summed) VLBI image can be rotated to match this. One needs to ensure a compact calibrator for this of course, which I would suggest would be your polarisation calibrator. This needs to be observed at several cuts of feed angle. Observations at zenith (where the feed angles for the Cassegrain antennae changes fastest) are to be encouraged. I have used the target, if it is strong enough, as the D-term calibrator.

VII   : Points of interest

VII.1   All

Pre-2008 versions of ATLOD would not retain the AN table, replacing with it with one appropriate for the Compact Array (i.e. linear polarisations). Versions of ATLOD post-Nov 2008 should handle these issues, as well as avoiding the "ATUV: FILE EXPANSION FAILED" bug.

VII.2   Hobart

Hobart has an EW-mount. It has a sister antennae, also a relocated ex-DSN tracking station, in Gilmore Creek, Alaska, with a North-South mount. The mount type in Hobart is now supported. For some of the receivers the feeds are linear, and converted to circulars with a Hybrid. This method has been shown to give D-terms less than 10%, should be stable over the experiment, but is not repeatable between sessions.

VII.3   ATCA

To include connected arrays such as ATCA is a huge advantage for any VLBI array, given that it can be internal calibrated to have zero D-terms. However if the antennae which form the phased array beam drift relative to each other this would be equivalent to a drifting D-term; this is not compatible with the AIPs approach to polarisation calibration. Therefore all VLBI experiments which wish to get good VLBI polarisation from ATCA should either use a single antenna, or continuously rephase the array (with CLCAL running continuously).

VII.4   Mopra

Mopra is a Cassegrain antenna, the only true Cassegrain antenna in the LBA. The feeds are linear, and are turned into circular signals via a hybrid. If the hybrid is not well tuned the system temperatures for the individual channels are very different. We should expect good D-terms from Mopra, if operating at the standard frequencies.

VII.5   Ceduna

Ceduna is a folded Cassegrain, which takes the same solution as for a true Cassegrain antenna. The feed are natively circular, as a quarter wave plate is part of the construction. D-terms in Ceduna have been seen to be reasonable.

VII.6   Parkes

Parkes is a Prime Focus, which takes the same solution as for a true Cassegrain antenna. Most of the feeds are converted to circular with hybrids, but not all. The D-terms from Parkes have been, at times, quiet high. Care should be taken in the set up for polarisation experiments with Parkes.

References

[1] R. Dodson, 2007, IT-OAN-2006-16, Informé Technico, "On the solution of the polarisation gain terms for VLBI data collected with antennae having Nasmyth or E-W mounts.".

[2] R. Dodson, 2008, AA, 480, 767, "First VLBI observations of methanol maser polarisation, in G339.88-1.26"

[3] M. Lister, D. Homan, 2005, AJ, 130, 138, "MOJAVE, 1. VLBA First-Epoch 15 GHz images"

A : Recommendations for calibration of polarisation observations

Many references have covered this, but here I wish to clearly layout the important steps in AIPS and the consequences of the tasks.

- **TABED** options: INE 'AN'; OPTY 'repl'; APARM 5 0 0 4 4 **3** and KEYV **5** 0
  Replaces the MNTSTA type of antenna 3 with value 5 (for a left handed Nasymth, such as Pico Veleta).
  For Hobart and the LBA this needs to be type 3. For data loaded with older versions of ATLOD this will need setting. Furthermore, in this case, one needs to change for all antenna: columns 8 and 11 to zero (APARM 8/11 0 0 2 0;KEYV 0), column 7 to 'R' and 10 to 'L' (APARM 7/10 0 0 3 0;KEYST 'R'/'L'). Recall also that Harts is Equatorial (mntyp 1).

- **CLCOR** options: CLCORP 1 0 and OPC 'pang'
  Calculates the phase correction for the listed mount types.

- **FRING** options: CALS 'prime_cal'; APARM(3)=0 and APARM(5)=0
  Finds the independent delays and combined rates and phases for the calibrator. Now the RR/LL phase will be constant.

- **CALIB** options: CALS 'prime_cal'; SOLMODE 'P'; APARM(3)=0 and APARM(5)=0
  Finds the independent rates and phases for the calibrator. Now the RR, LL and RR/LL phases will be zero. One may wish to use only one scan on the prime calibrator.

- **VLBACPOL** this procedure finds the delays between left and right hand for the reference antenna. If PCAL (or something similar) is used the delay between left and right should be zero.

- **FRING** options: CALS 'target','calib'; APARM(3)=1 and APARM(5)=1
  Finds the rates and combined phases for the target.

- **CALIB** options: CALS 'calib'; SOLMODE 'A&P'; APARM(3)=1 and APARM(5)=1
  Produces a well calibrated version of the target which can be imaged.

- **IMAGR** Deconvolve this with, either a few model components, or clean it and then box up the clean components into a few regions (with CCEDT), and use it for the next stage.

- **LPCAL** options: CALS 'calib'; in2na 'calib' and in2c 'icln'
  Does the polarisation calibration on the target, using the cleaned model.

- **CALIB** options: CALS 'target'; SOLMODE 'A&P'; DOPOL 2; APARM(3)=1 and APARM(5)=1
  Calibrates the target using the polarisation solutions.

- **IMAGR** Image the source in I, Q and U. The sum of the fluxes (total and polarised) should compare to the lower resolution (VLA or ATCA) values. The correction ϕ_{RL} is $2\chi_{\mathrm{true}} - \arctan(\frac{\sum \mathrm{U}}{\sum \mathrm{Q}})$, for each IF.

- **CLCOR** options: CLCORP ϕ_{RL} stokes 'L' and OPC 'polr'
  Rotates the D-terms to match the calibration value of χ_{true}.

If this recipe is not followed the solutions for the L and R hand polarisations are independent. This is not a problem if there is sufficient signal to noise, however in mm-VLBI this is rarely the case and the two polarisations need to be combined in the fringe search stage. This is why it is important not to treat them as independent except for the prime calibrator.

B : A list of the changes to classic AIPS

A summary of the files changed:

- LPCAL.FOR: Add a new subroutine LPCAL_VIS

- LPCAL_EXT.FOR: New program to allow dual D-terms

- PARANG.FOR: all mount types now supported

- PRTAN.FOR: Add mount names

- CLCOR.FOR: in ANAXIS allow all mount types

- APCAL.FOR: in AMPCAL allow all mount types

- DFCOR.FOR: in ANAXIS allow all mount types

- SNPLT.FOR: does not use PARANG, so mount types added

- DTSIM.FOR: (in ORIENT) does not use PARANG, so mount types added

- DTSIM.FOR: (in GETBAS) allow all mount types